

## White Dwarf Structure and Binary Inspiral Gravitational Waves from Quantum Hadrodynamics

LING-JUN GUO,<sup>1,2</sup> YAO MA,<sup>1,3</sup> YONG-LIANG MA,<sup>3,4</sup> RUO-XI WU,<sup>1,5,6</sup> AND YUE-LIANG WU<sup>1,4,5,7</sup>

<sup>1</sup>*School of Fundamental Physics and Mathematical Sciences, Hangzhou Institute for Advanced Study, UCAS, Hangzhou, 310024, China*

<sup>2</sup>*College of Physics, Jilin University, Changchun, 130012, China*

<sup>3</sup>*School of Frontier Sciences, Nanjing University, Suzhou 215163, China*

<sup>4</sup>*International Center for Theoretical Physics Asia-Pacific (ICTP-AP), UCAS, Beijing, 100190, China*

<sup>5</sup>*Institute of Theoretical Physics, Chinese Academy of Sciences, Beijing, 100190, China*

<sup>6</sup>*University of Chinese Academy of Sciences, Beijing, 100049, China*

<sup>7</sup>*TaiJi Laboratory for Gravitational Wave Universe (Beijing/Hangzhou), University of Chinese Academy of Sciences, Beijing, 100049, China*

(Dated: October 10, 2024)

### ABSTRACT

White dwarf, one of the compact objects in the universe, is not only pivotal for astrophysical inquiries but also furnishes a dynamic arena for nuclear physics exploration. In this work, we extend the relativistic mean field approach using a Walecka-type quantum hadrodynamics model to encapsulate the intricate structure of white dwarfs. This methodological advancement facilitates a cohesive analysis of white dwarfs, neutron stars, and the nuclear pasta within a unified theoretical framework. By meticulously calibrating the model parameters to nuclear matter properties, we successfully replicate the structures of various nuclei, such as <sup>4</sup>He, isotopes of C, and <sup>16</sup>O. Subsequently, we predict the properties of white dwarfs composed of atom-like units and the gravitational waves stemming from binary white dwarf inspirals incorporating tidal deformability contributions up to the 2.5 post-Newtonian order. These results shed light on the structure of white dwarfs and offer more clues for future gravitational wave detection.

### 1. INTRODUCTION

The detection of gravitational waves (GWs) by the LIGO/Virgo Collaborations [Abbott et al. \(2016, 2017, 2019\)](#) signifies that astronomy has entered the era of multi-messenger observations, providing a new means to probe the nature of compact objects such as black holes (BHs) and neutron stars (NSs). The space-based detectors like LISA [Amaro-Seoane et al. \(2017\)](#), Taiji [Hu & Wu \(2017\)](#), and TianQin [Luo et al. \(2016\)](#) which are scheduled to be launched in the 2030s aim to the GWs with frequency 0.1mHz-0.1Hz. One of the sources of these space-based low-frequency GW detectors is the white dwarf (WD) binaries [Ruiter et al. \(2010\)](#); [Yu & Jeffery \(2010\)](#); [Tamanini & Danielski \(2019\)](#); [McNeill et al. \(2020\)](#); [Wolz et al. \(2020\)](#); [Korol et al. \(2020\)](#); [Gibney \(2024\)](#)—another kind of compact object in the universe.

In addition to their astronomical significance, WDs have profound implications for nuclear physics. Binary WDs are intimately connected to Type Ia supernova (SN) explosions, events rich in physics involving strong interaction, weak interaction, and intense electromagnetic fields [Niemeyer & Woosley \(1997\)](#); [Jose & Hernanz \(1998\)](#); [Fryer et al. \(1999\)](#); [Rosswog et al. \(2009\)](#); [Toonen et al. \(2012\)](#); [Katz & Dong \(2012\)](#); [Kashiyama et al. \(2013\)](#). Understanding the structure of WDs, especially the components of the cores of WDs, is a complex yet crucial task for nuclear physics,

[mayao@ucas.ac.cn](mailto:mayao@ucas.ac.cn)

[ylma@nju.edu.cn](mailto:ylma@nju.edu.cn)

[ylwu@ucas.ac.cn](mailto:ylwu@ucas.ac.cn)

and GWs from binary WD systems provide valuable insights into the characteristics of the internal structure of WDs and therefore the nuclear forces [McNeill et al. \(2020\)](#); [Saumon et al. \(2022\)](#).

In the description of nuclear force, the quantum hadrodynamics (QHD) written in terms of colorless hadrons plays an indispensable role [Walecka \(1974\)](#); [Serot & Walecka \(1986\)](#); [Weinberg \(1990\)](#); [Serot & Walecka \(1997\)](#). In the realm of hadron interactions, linear and non-linear realizations of chiral symmetry stand out as frameworks that more directly mirror QCD properties [Weinberg \(1979, 1990\)](#); [Gasser et al. \(1988\)](#); [Bando et al. \(1985, 1988\)](#); [Harada & Yamawaki \(2003\)](#), offering an alternative to the traditional Walecka-type parametrization. With respect to the flavor or chiral symmetry, the electromagnetic and weak forces can be self-consistently included. Therefore, QHD is a unified framework for nucleon, nuclei, and their electromagnetic and weak processes.

In this work, anchored on the Walecka-type QHD, we extend the relativistic mean field (RMF) approach which has been widely use in the study of homogeneous nuclear matter (NM) and NM clusters [Watanabe et al. \(2000\)](#); [Horowitz et al. \(2005\)](#); [Xia et al. \(2022\)](#); [You et al. \(2024\)](#) to study WD properties. The WDs are suggested to be made of charge-neutral objects—atom-like units—which have finite nucleon number nucleons within a box surrounded by an electron cloud. These objects effectively replicate the Wigner-Seitz cell structure of WDs [Salpeter \(1961\)](#); [Rotondo et al. \(2011a\)](#). The approach developed here can be taken as the microscopic materialization of the phenomenological parameterization of EOS of WD matter, such as the Thomas-Fermi model and Feynman-Metropolis-Teller (FMT) model [Feynman et al. \(1949\)](#); [Rotondo et al. \(2011b\)](#). The primary advantage of this extension is the ability to describe NSs, NS crusts, and WDs within a singular framework by utilizing a consistent set of interaction parametrizations, facilitating seamless transitions between modeling binary NSs, WDs, and NS-WD systems.

Utilizing the above extension, we calculate the properties of  ${}^4\text{He}$ , isotopes of C and  ${}^{16}\text{O}$  with the parameters of the model meticulously fitted by the properties of NM and the structural characteristics of NSs. Then, we deduce the structures of WDs, e.g., mass-radius (M-R) relation and tidal deformability (TD), composed of different elements ( ${}^4\text{He}$ ,  ${}^{12}\text{C}$ , and  ${}^{16}\text{O}$ ). Finally, we study the GW signals stemming from the inspirals of the binary WDs with and without TD through the application of the post-Newtonian (PN) approximation [Cutler et al. \(1993\)](#); [Damour et al. \(2001\)](#) at the 2.5PN order. Our results of the WDs made of  ${}^4\text{He}$ , isotopes of C and  ${}^{16}\text{O}$  are consistent with the observation data and Chandrasekhar limit, where free electron gas is assumed, and the GW signals stemming from the binary WDs composed of different elements are investigated. These results can serve as preliminary guides for future GW detection, offering insights into the nuances of binary WD dynamics.

The rest of this paper is organized as follows: Sec. 2 introduces the framework of the extended RMF method and presents numerical results pertaining to the properties of NM and nuclei. Sec. 3 explores the structures of WDs and simulates the GW signals resulting from binary WD inspirals. Our discussion and outlook are given in the last section. We devote ourselves to the structure of nuclei and the EOS of WDs in Appendix A and the detail of PN expansion in Appendix B.

## 2. THE EXTENDED RMF AND NUCLEUS

Without loss of generality, we consider a Walecka-type model which has been widely used in nuclear physics [Sugahara & Toki \(1994\)](#); [Shen et al. \(1998\)](#). Including electromagnetic (EM) interaction, the model is written as:

$$\mathcal{L} = \mathcal{L}_{\text{fermion}} + \mathcal{L}_{\text{boson}} + \mathcal{L}_I, \quad (1)$$

where

$$\begin{aligned} \mathcal{L}_{\text{fermion}} &= \bar{\Psi} (i\not{D} - m_N) \Psi + \bar{\psi} (i\not{D} - m_e) \psi, \\ \mathcal{L}_{\text{boson}} &= \frac{1}{2} (\partial_\mu \sigma \partial^\mu \sigma - m_\sigma^2 \sigma^2) - \frac{1}{3} g_2 \sigma^3 - \frac{1}{4} g_3 \sigma^4 \\ &\quad - \frac{1}{4} \Omega_{\mu\nu} \Omega^{\mu\nu} + \frac{1}{2} m_\omega^2 \omega_\mu \omega^\mu + \frac{1}{4} c_3 (\omega_\mu \omega^\mu)^2 \\ &\quad - \frac{1}{4} \vec{P}_{\mu\nu} \cdot \vec{P}^{\mu\nu} + \frac{1}{2} m_\rho^2 \vec{\rho}_\mu \cdot \vec{\rho}^\mu - \frac{1}{4} F_{\mu\nu} F^{\mu\nu}, \\ \mathcal{L}_I &= \bar{\Psi} (-g_\sigma \sigma - g_\omega \not{\omega} - g_\rho \vec{\rho}) \Psi, \end{aligned} \quad (2)$$

with  $\Psi = \begin{pmatrix} p \\ n \end{pmatrix}$  and  $\psi$  being, respectively, nucleon iso-doublet and electron fields.  $A_\mu$  is the EM field,  $\sigma, \omega_\mu$  and  $\vec{\rho}_\mu = \rho_\mu^i \tau^i$  (with  $\tau_i$  being the Pauli matrix) are isoscalar-scalar, isoscalar-vector and isovector-vector meson fields, respectively.

The pseudoscalar mesons  $\pi$  are neglected since they vanish in the RMF approximation.  $\vec{P}_{\mu\nu} = D_\mu \vec{\rho}_\nu - D_\nu \vec{\rho}_\mu$  is the field-strength tensor of rho meson fields. The covariant derivatives are defined as

$$\begin{aligned} D_\mu \Psi &= (\partial_\mu + iA_\mu Q) \Psi , \\ D_\mu \psi &= (\partial_\mu - ieA_\mu) \psi , \\ D_\mu \vec{\rho}_\nu &= \partial_\mu \vec{\rho}_\nu + iA_\mu [Q, \vec{\rho}_\nu] , \end{aligned} \quad (3)$$

where the charge matrix  $Q = e(1 + \tau_3)/2$  with  $\tau_3$  being the third component of Pauli matrices.

By taking appropriate boundary conditions (BCs), the homogeneous NM and NM clusters can be calculated using the standard RMF approach [Watanabe et al. \(2000\)](#); [Horowitz et al. \(2005\)](#); [Xia et al. \(2022\)](#). However, these BCs cannot be naively extended to the WD matter since the repulsive force from the EM interaction is much stronger than the attractive nuclear force. Here, we propose that the WD is made of atom-like units which have a nucleus core surrounded by homogeneous electron gas, as depicted in Fig. 1. For simplicity, we assume that both WD and its constitute unit are spherically symmetric.

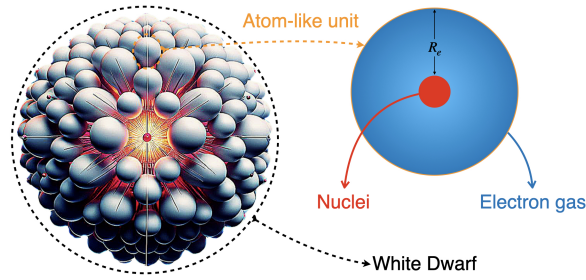


**Figure 1.** The carton of WDs. WDs are composed of atom-like units with a single nuclei inside and the nuclei are surrounded by electron gas.

Then, homogeneous condition degenerates into isotropy so that the time derivatives and spatial components of meson fields can be neglected. The equations of motion (EOMs) to be solved are

$$\begin{aligned} -\nabla^2 A &= en_p - en_e , \\ (-\nabla^2 + m_\rho^2) \rho &= g_\rho (n_p - n_n) , \\ (-\nabla^2 + m_\omega^2) \omega &= g_\omega (n_p + n_n) + c_3 \omega^3 , \\ (-\nabla^2 + m_\sigma^2) \sigma &= -g_\sigma (n_n^s + n_p^s) - g_2 \sigma^2 - g_3 \sigma^3 , \end{aligned} \quad (4)$$

where  $n_i$  and  $n_i^s$  are, respectively, the number density and scalar density of particle “ $i$ ”, and the scalar density

$$n_{n(p)}^s = \frac{m_N^{*3}}{\pi^2} \left[ \frac{1}{2} \left( t_{n(p)} \sqrt{1 + t_{n(p)}^2} - \operatorname{arcsinh} t_{n(p)} \right) \right] , \quad (5)$$

with  $t_{n(p)} = \frac{(3\pi^2 n_{n(p)})^{1/3}}{m_N^*}$  and  $m_N^* = m_N + g_\sigma \sigma$  defined by EOMs of fermions:

$$\begin{aligned} (i\cancel{\partial} - m_N - g_\sigma \sigma - g_\rho \rho \gamma^0 \tau^3 - g_\omega \omega \gamma^0 - A \gamma^0 Q) \Psi &= 0 , \\ (i\cancel{\partial} - m_e + eA) \psi &= 0 . \end{aligned} \quad (6)$$

Note that in Eq. (4) only the zeroth component of the vector meson fields are considered and the component indices are omitted. By using the EOMs (4) and (6), the Hamiltonian (energy) density can be obtained via Legendre transformation from (1) in a straightforward way.

To study the structure of nuclei inside the atom-like unit using model (1), we adopt the parameter values listed in Tab. 1 which were obtained by meticulously calibrating to align with the properties of NM and the M-R relations

of NSs Guo et al. (2024). The nuclei are assumed to be spherical, and energy density can be calculated by ignoring the contribution from electrons. In our calculation, the initial distribution of fields are set to be within a sphere with radius  $R = 5$  fm, and the EOM (4) is iteratively solved to find the ground state of corresponding nuclei. Our results of the nuclei properties are shown in Tab. 2.

**Table 1.** Optimal values of the parameters obtained from pinning down NM properties and NS star structures Guo et al. (2024).

$g_\sigma$	$g_\omega$	$g_\rho$	$g_3$	$c_3$	$g_2$	$m_\sigma$
9.82	11.8	3.42	1.26	72.6	-1550 MeV	531 MeV

**Table 2.** The results of nuclei properties. The root-mean-square radius  $\sqrt{\langle r^2 \rangle}$  is calculated via  $\langle r^2 \rangle = \int_0^{R_0} R^2 \rho(R) 4\pi R^2 dR / \int_0^{R_0} \rho(R) 4\pi R^2 dR$ , where  $\rho(R)$  is the distribution of nucleons of the ground state and  $R_0$  is the appropriate truncation for corresponding integral. The binding energy B.E. is defined by  $m_N - E_i / (N + Z)$ , where “ $i$ ” refers to different elements with  $N(Z)$  being the number of neutron (proton) inside the nuclei. The empirical values (denoted as “Emp.”) are taken from Refs. Fortune (2016); National Nuclear Data Center (2024); Pössel (2010). The radius  $\sqrt{\langle r^2 \rangle}$  and B.E. are in the units of fm and MeV, respectively.

Elements	${}^4\text{He}$	${}^{12}\text{C}$	${}^{13}\text{C}$	${}^{14}\text{C}$	${}^{15}\text{C}$	${}^{16}\text{C}$	${}^{17}\text{C}$	${}^{18}\text{C};$	${}^{19}\text{C}$	${}^{20}\text{C}$	${}^{16}\text{O}$
$\sqrt{\langle r^2 \rangle}$ (Emp.)	-	-	-	2.33(7)	2.54(4)	2.74(3)	2.76(3)	2.86(4)	3.16(7)	2.98(5)	-
$\sqrt{\langle r^2 \rangle}$ (The.)	1.72	2.24	2.30	2.35	2.41	2.47	2.54	2.60	2.66	2.72	2.43
B.E. (Emp.)	7.07	7.68	7.47	7.52	7.10	6.92	6.56	6.43	6.12	5.96	7.98
B.E. (The.)	4.29	7.17	7.33	7.35	7.28	7.14	6.96	6.75	6.52	6.29	7.82

From Tab. 2, one can see that our current approach successfully captures the qualitative properties of nuclei, except the B.E. of  ${}^4\text{He}$ , which is unnaturally deep bounded, see Ref. Beane et al. (2013). Additionally, the results increasingly diverge from empirical data with  $N - Z$ . This deviation is attributed to the oversimplified parametrization of isospin-related interactions, especially those involving the  $\rho$  meson.

### 3. THE STRUCTURE OF WHITE DWARFS AND BINARY INSPIRALS

The energy density  $\mathcal{E}$  of the atom-like units can be calculated by using model (1) and pressure can be obtained through

$$P = -\mathcal{E} + \mathcal{N} \frac{d\mathcal{E}}{d\mathcal{N}}, \quad (7)$$

where  $\mathcal{N}$  is density of the atom-like unit number. It should be noted that the pure mesonic parts of energy density disappear outside the nuclei. Our numerical results of nucleon density distributions of different nuclei and the corresponding EOS of WD matter are shown in App. A.

#### 3.1. Structure of white dwarf

After obtaining  $\mathcal{E} - P$  relation, the M-R relations can be calculated by solving the Tolman-Oppenheimer-Volkoff (TOV) equations Tolman (1939); Oppenheimer & Volkoff (1939) and the TD of WDs can also be obtained following Ref. Flanagan & Hinderer (2008). It should be noted that in our present work, we will not concern about the effect of  $\beta$ -equilibrium Salpeter (1961); Rotondo et al. (2011b,a); Boshkayev et al. (2013). Our results are shown in Fig. 2, where it can be seen that our WD structures saturate the regular Chandrasekhar limit (free electron gas, a pivotal concept in astrophysics). A comparison of the pressure at different mass density obtained from our approach, Chandrasekhar limit, Salpeter approach, and the relativistic FMT from Ref. Rotondo et al. (2011a) are shown in Table 3. It can be seen that, in our approach, the structure of WDs is consistent with the Salpeter approach and the relativistic FMT framework, which slightly deviates from the Chandrasekhar limit. Our results align well within the region of the

observational data, thereby validating the effectiveness of our theoretical framework in describing the properties of WDs.

**Table 3.** The pressure at different mass densities  $\rho_{\text{mass}}$  for regular Chandrasekhar limit ( $P_{\text{Ch}}$ ), Salpeter approach ( $P_{\text{S}}$ ), the relativistic FMT ( $P_{\text{FMT}}^{\text{rel}}$ ), our parametrization with free electron gas limit ( $P_{\text{RMF}}^{\text{Ch}}$ ), and our parametrization ( $P_{\text{RMF}}$ ).  $\rho_{\text{mass}}$  is unit of  $\text{g}/\text{cm}^3$ , and pressure is in the unit of  $\text{dyne}/\text{cm}^2$ . We take  $^{12}\text{C}$  as an example.

$\rho_{\text{mass}}$	$P_{\text{Ch}}$	$P_{\text{S}}$	$P_{\text{FMT}}^{\text{rel}}$	$P_{\text{RMF}}^{\text{Ch}}$	$P_{\text{RMF}}$
$10^4$	$1.45 \times 10^{19}$	$1.29 \times 10^{19}$	$1.29 \times 10^{19}$	$1.45 \times 10^{19}$	$1.29 \times 10^{19}$
$10^5$	$6.50 \times 10^{20}$	$6.14 \times 10^{20}$	$6.13 \times 10^{20}$	$6.48 \times 10^{20}$	$6.13 \times 10^{20}$
$10^6$	$2.63 \times 10^{22}$	$2.55 \times 10^{22}$	$2.54 \times 10^{22}$	$2.62 \times 10^{22}$	$2.54 \times 10^{22}$
$10^7$	$8.46 \times 10^{23}$	$8.29 \times 10^{23}$	$8.27 \times 10^{23}$	$8.44 \times 10^{23}$	$8.28 \times 10^{23}$
$10^8$	$2.15 \times 10^{25}$	$2.11 \times 10^{25}$	$2.11 \times 10^{25}$	$2.14 \times 10^{25}$	$2.11 \times 10^{25}$
$10^9$	$4.86 \times 10^{26}$	$4.78 \times 10^{26}$	$4.77 \times 10^{26}$	$4.84 \times 10^{26}$	$4.77 \times 10^{26}$
$10^{10}$	$1.06 \times 10^{28}$	$1.04 \times 10^{28}$	$1.04 \times 10^{28}$	$1.05 \times 10^{28}$	$1.04 \times 10^{28}$

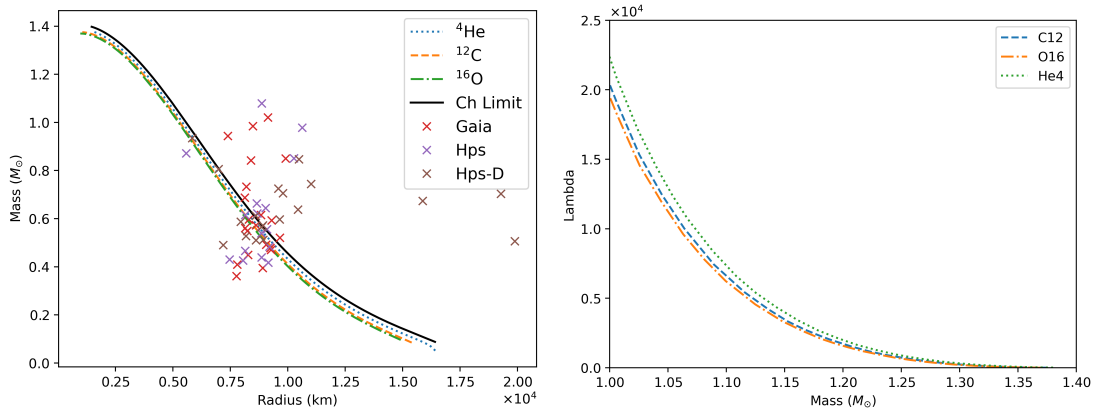


**Figure 2.** The M-R relation (left panel) and TD (right panel) of WDs. The observational data marked by "x" are taken from Ref. Tremblay et al. (2016). The Chandrasekhar limit of our parametrization (denoted as 'Ch') is also plotted for comparison.

### 3.2. Gravitational waves of binary inspirals

We finally calculate the GW signals from the binary WD inspirals with and without tidal deformability at the 2.5PN order. The expression of the GW waveforms up to 2.5PN order are listed in the App. B. The results of the GWs from binary WDs composed of different elements in frequency-domain, are shown in Fig. 3 and Fig. 4 for, respectively, the phase shift and amplitude deviation. We typically choose the equal mass system with component mass  $1.1 M_{\odot}$ . The corresponding tidal deformability are  $\Lambda = 7352, 6613, 6197$  for  $^4\text{He}$ ,  $^{12}\text{C}$ , and  $^{16}\text{O}$ , respectively, according to the results of Fig. 2.

Our results illustrated Fig. 3 and Fig. 4 indicate that WDs composed of lighter elements show a bigger deviation from the point-particle approximation—the GW signals without TD—in terms of both phase and amplitude, in line with the tidal deformability shown in Fig. 2. Although the PN approximation may not be suitable for the merging stage of WD inspirals, particularly in the hundred Hz frequency range, the discernible differences between the point particle approximation and the tidal deformability corrections offer a preliminary understanding of matter effects on GWs. This is especially valuable given the complexities involved in numerical simulations for such systems. Comparative analyses in both the mHz and hundred Hz regions could serve as initial guides for future GW detections and as a testbed for further research on WDs. Moreover, understanding the point particle approximation's limitations in GW physics is essential for interpreting GW signals accurately.

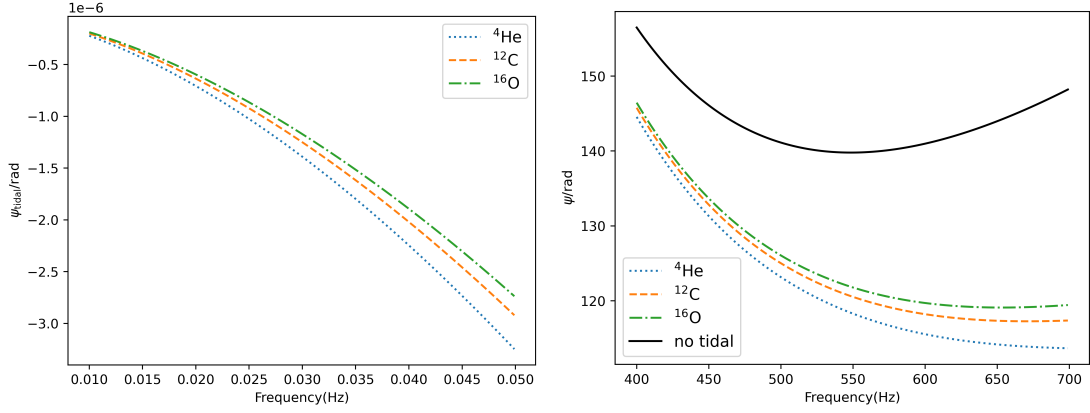


**Figure 3.** The phase shift of GWs in mHz region (left panel) and hundred Hz region (right panel).

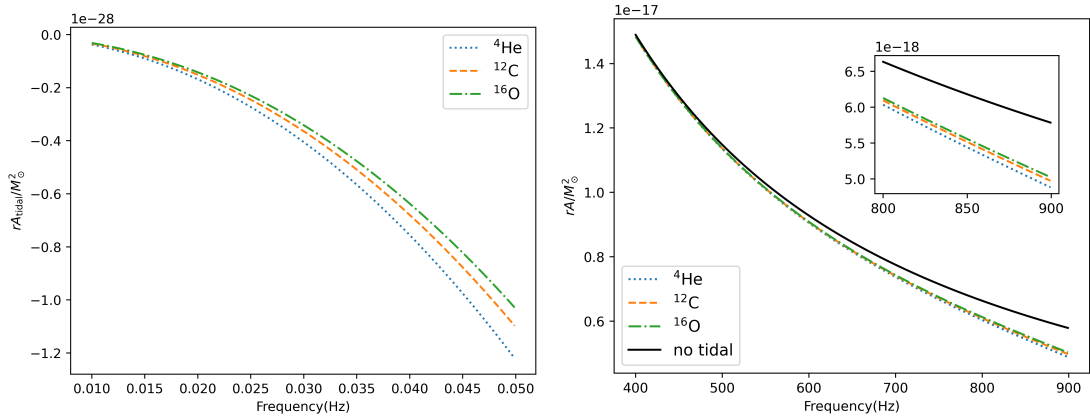


**Figure 4.** The amplitude deviation of GWs in mHz region (left panel) and hundred Hz region (right panel) introduced by TD.

Our results of the dimensionless characteristic strain amplitude  $h_c(f)$  Moore et al. (2015)

$$h_c(f) = \sqrt{f S_h(f)} = 2f |\tilde{h}(f)| \quad (8)$$

in comparison with the detectabilities of LISA Belgacem et al. (2019), Taiji Luo et al. (2020, 2021), and TianQin Gong et al. (2021), at  $r = 3\text{Mpc}$  and  $300\text{Mpc}$ , are presented in Fig. 5. One can see that, as expected, the events of the inspirals at  $\gtrsim 300\text{Mpc}$  are indeed detectable by these space-based facilities.

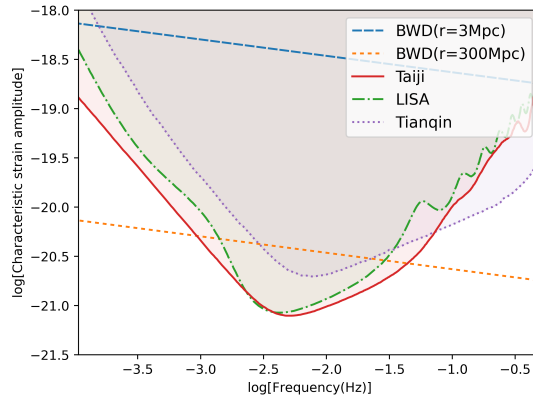


**Figure 5.** The predicted characteristic strain amplitude of GWs in comparison with the detectabilities of space-based facilities.

#### 4. SUMMARY AND PERSPECTIVE

In this work, we successfully extended the RMF approach to study the WDs and proposed an atom-like constituent of WDs. The achieved properties of nuclei and WDs are closely aligned with observational data. The GWs stemming from the merger of binary WDs are also studied. A notable advantage of our approach is the ability to describe NSs, NS crusts, and WDs within a single, cohesive framework by employing distinct BCs.

Upon the parameters established from the properties of ordinary homogeneous NM at saturation density, we proceeded to determine the structure of nuclei. The results obtained are closely aligned with empirical data [Fortune \(2016\)](#); [National Nuclear Data Center \(2024\)](#); [Pössel \(2010\)](#), except for the anomalously deep bounded  ${}^4\text{He}$  and nuclei with large neutron-proton ( $N - Z$ ) differences, which are attributed to the simplified interaction parametrizations. Subsequently, we computed the M-R relations and TD of WDs conceptualizing them as an atom-like unit composed objects and found that the yielded results are in concordance with observational data [Tremblay et al. \(2016\)](#). This congruence underscores the efficacy of our model in capturing the essential physics of WDs.

Finally, we generated GW signals for binary WD inspirals composed of various elements,  ${}^4\text{He}$ ,  ${}^{12}\text{C}$ , and  ${}^{16}\text{O}$ , considering both scenarios with and without TD across mHz and hundred Hz frequency ranges, up to the 2.5 PN order. The resulting signals indicate that WDs composed of lighter elements exhibit bigger deviations from the point particle approximation, consistent with the TD findings. These results provide valuable preliminary guidelines for interpreting future GW detection signals.

We should say that the model used and the structure of WDs considered in this work are immature. Several improvements deserve further consideration:

Firstly, as well known, the present used Walecka-type model is not enough for precisely describe nuclei and NM. So that it is interesting to fine the calculation using more realistic models anchored on the chiral symmetry of QCD [Jenkins & Manohar \(1991\)](#); [Bernard \(2008\)](#); [Scherer \(2010\)](#); [Ma & Ma \(2024\)](#); [Li et al. \(2017\)](#); [Ma & Rho \(2017\)](#), ab initio parameterized nuclear force [Bender et al. \(2003\)](#); [Stoitsov et al. \(2010\)](#); [Hergert et al. \(2016\)](#); [Duguet et al. \(2015\)](#) or Skyme force parameterization [Agrawal et al. \(2006\)](#); [Lesinski et al. \(2006\)](#); [Zuo et al. \(2018\)](#). We expect these studies can advance our grasp of the interplay between nuclear structure physics and QCD and access to nuclei structure more precisely.

Secondly, so far we suppose that the WDs are made up of the atom-like units with a fixed nuclei. To take the shell structure of WDs into account, the transition between elements should be properly considered in the future work.

Thirdly, although this preliminary work catches the dominant physics of WD, we only considered the WD made of a unique nucleus. It is accepted that the inverse beta-decay of nucleus plays a fundamental role in WD physics [Rotondo et al. \(2011b,a\)](#); [Boshkayev et al. \(2013\)](#). This deserves a serious consideration in the present framework.

#### ACKNOWLEDGMENTS

Y. L. M. would like to thank C. J. Xia for his valuable discussion. The work of Y. L. M. was supported in part by the National Key R&D Program of China under Grant No. 2021YFC2202900 and the National Science Foundation of China (NSFC) under Grant No. 12347103 and No. 11875147. Y. L. W. was supported in part by the National Key Research and Development Program of China under Grant No.2020YFC2201501, the National Science Foundation of China (NSFC) under Grants No. 12347103, No. 12147103, No. 11821505, and the Strategic Priority Research Program of the Chinese Academy of Sciences under Grant No. XDB23030100.

#### APPENDIX

##### A. THE NUCLEI STRUCTURES AND EOS OF WHITE DWARFS

Our results of the nucleon density distribution in an isotope and EOS of WDs are plotted, respectively, in [Fig. 6](#) and [Fig. 7](#).

##### B. THE POST-NEWTONIAN EXPANSION UP TO THE 2.5PN ORDER

The GW in the frequency-domain ( $f$ ) can be obtained via [Husa et al. \(2016\)](#); [Isoyama et al. \(2020\)](#),

$$\tilde{h}(f) = \int h(t) e^{i2\pi ft} dt = A(f) e^{i(\psi_{\text{SPA}}(f) - \pi/4)}, \quad (\text{B1})$$

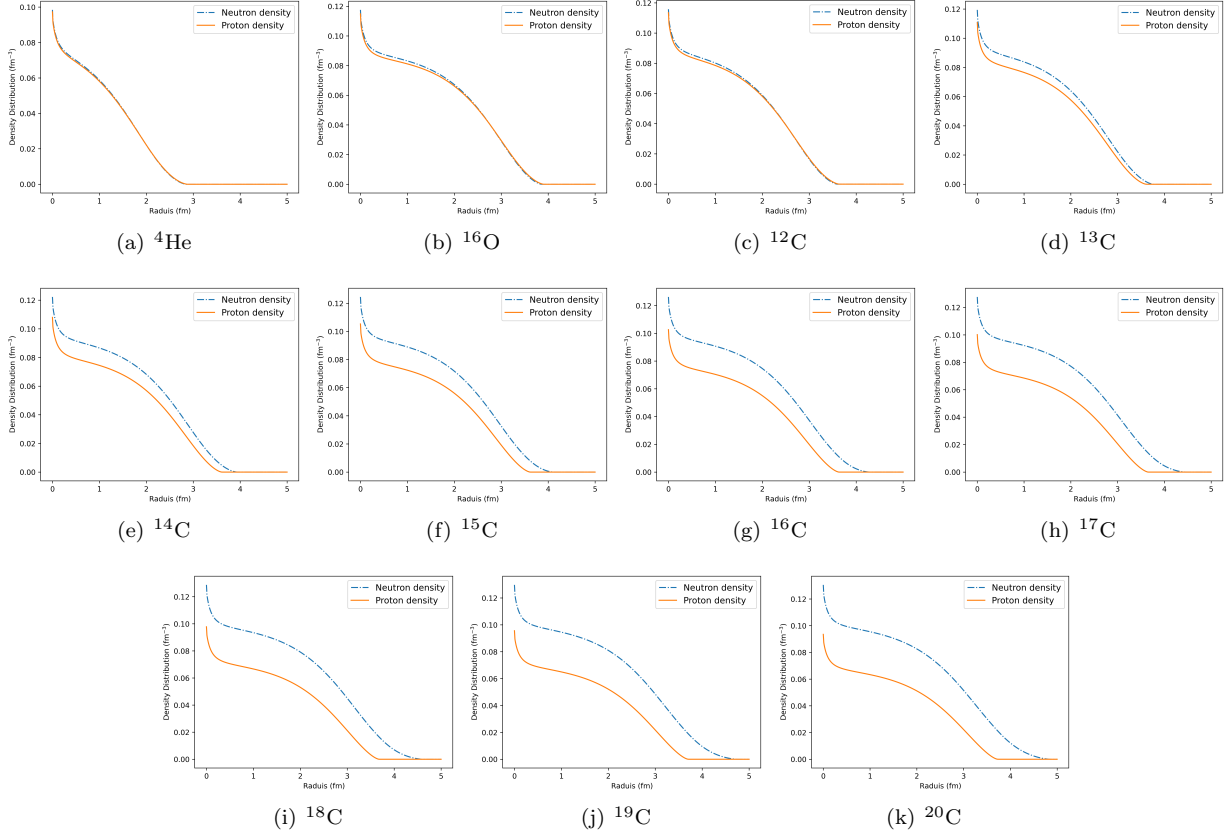
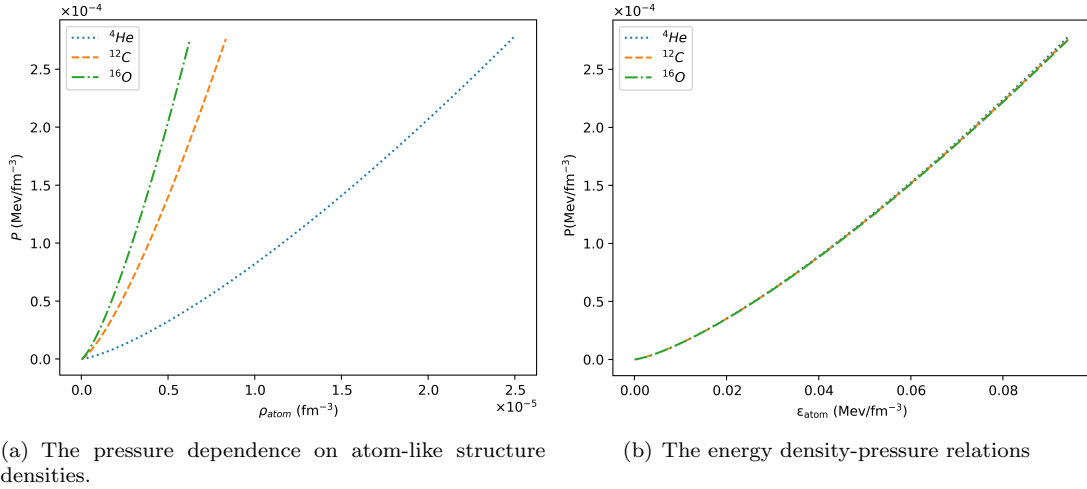


**Figure 6.** The nucleon density distributions of ground states of different kinds of nuclei.



(a) The pressure dependence on atom-like structure densities.

(b) The energy density-pressure relations

**Figure 7.** The EOS of WDs composed of different elements.

where  $\psi_{\text{SPA}}(f) = 2\pi f t(f) - \psi(f)$ .  $\psi(f)$  can be decomposed into point and tidal parts as  $\psi(f) = \psi_{\text{pp}}(f) + \psi_{\text{tidal}}(f)$  and the same treatment can be applied to amplitude  $A(f) = A_{\text{pp}}(f) + A_{\text{tidal}}(f)$ . The explicit expressions for the amplitude and phase are [Isoyama et al. \(2020\)](#); [Buonanno et al. \(2009\)](#); [Kawaguchi et al. \(2018\)](#)

$$A_{\text{pp}}(f) \simeq \frac{\mathcal{M}^{5/6}}{r} \sqrt{\frac{2}{3\pi^{1/3}}} f^{-7/6} \left( 1 + O\left(f^{2/3}\right) \right), \quad (\text{B2})$$



where  $\mathcal{M} = M\nu^{3/5}$  is the chirp mass with  $M = m_1 + m_2$ ,  $\nu = m_1 m_2 / M^2$ , and  $r$  being the observation distance. Meanwhile,

$$A_{\text{tidal}}(f) = \sqrt{\frac{5\pi\nu}{24} \frac{M^2}{r}} \tilde{\Lambda} v^{-7/2} \left( -\frac{27}{16} v^{10} - \frac{449}{64} v^{12} - 4251 v^{15.780} \right), \quad (\text{B3})$$

where  $\tilde{\Lambda} = \frac{16}{13} \frac{(m_1+12m_2)m_1^4\Lambda_1+(m_2+12m_1)m_2^4\Lambda_2}{M^5}$  is the tidal formation of inspirals,  $v = (\pi M f)^{1/3}$ . Moreover,

$$\begin{aligned} \psi_{\text{pp}}(f) = & 2\pi f t_c - \phi_c - \frac{\pi}{4} + \frac{3}{128\nu v^5} \left[ 1 + \frac{20}{9} \left( \frac{743}{336} + \frac{11}{4}\nu \right) v^2 - 16\pi v^3 \right. \\ & \left. + 10 \left( \frac{3058673}{1016064} + \frac{5429}{1008}\nu + \frac{617}{144}\nu^2 \right) v^4 + \pi \left( \frac{38645}{756} - \frac{65}{9}\nu \right) \left\{ 1 + 3 \log \left( \frac{v}{v_{\text{iso}}} \right) \right\} v^5 \right] \end{aligned} \quad (\text{B4})$$

where  $t_c$  and  $\phi_c$  are chosen to be zero, meanwhile  $v_{\text{iso}} = \sqrt{6}$  is the last-stable-orbit termination condition defined by the Schwarzschild metric, and

$$\psi_{\text{tidal}}(f) = \frac{3v^5}{128\nu} \left[ -\frac{39}{2} \tilde{\Lambda} \left( 1 + 12.55 \tilde{\Lambda}^{2/3} v^{8.480} \right) \right] \times \left( 1 + \frac{3115}{1248} v^2 - \pi v^3 + \frac{28024205}{3302208} v^4 - \frac{4283}{1092} \pi v^5 \right). \quad (\text{B5})$$

## REFERENCES

- Abbott, B. P., et al. 2016, *Phys. Rev. Lett.*, 116, 061102, doi: [10.1103/PhysRevLett.116.061102](https://doi.org/10.1103/PhysRevLett.116.061102)
- . 2017, *Phys. Rev. Lett.*, 119, 161101, doi: [10.1103/PhysRevLett.119.161101](https://doi.org/10.1103/PhysRevLett.119.161101)
- . 2019, *Phys. Rev. X*, 9, 031040, doi: [10.1103/PhysRevX.9.031040](https://doi.org/10.1103/PhysRevX.9.031040)
- Agrawal, B. K., Dhiman, S. K., & Kumar, R. 2006, *Phys. Rev. C*, 73, 034319, doi: [10.1103/PhysRevC.73.034319](https://doi.org/10.1103/PhysRevC.73.034319)
- Amaro-Seoane, P., et al. 2017, <https://arxiv.org/abs/1702.00786>
- Bando, M., Kugo, T., Uehara, S., Yamawaki, K., & Yanagida, T. 1985, *Phys. Rev. Lett.*, 54, 1215, doi: [10.1103/PhysRevLett.54.1215](https://doi.org/10.1103/PhysRevLett.54.1215)
- Bando, M., Kugo, T., & Yamawaki, K. 1988, *Phys. Rept.*, 164, 217, doi: [10.1016/0370-1573\(88\)90019-1](https://doi.org/10.1016/0370-1573(88)90019-1)
- Beane, S. R., Chang, E., Cohen, S. D., et al. 2013, *Phys. Rev. D*, 87, 034506, doi: [10.1103/PhysRevD.87.034506](https://doi.org/10.1103/PhysRevD.87.034506)
- Belgacem, E., et al. 2019, *JCAP*, 07, 024, doi: [10.1088/1475-7516/2019/07/024](https://doi.org/10.1088/1475-7516/2019/07/024)
- Bender, M., Heenen, P.-H., & Reinhard, P.-G. 2003, *Rev. Mod. Phys.*, 75, 121, doi: [10.1103/RevModPhys.75.121](https://doi.org/10.1103/RevModPhys.75.121)
- Bernard, V. 2008, *Prog. Part. Nucl. Phys.*, 60, 82, doi: [10.1016/j.ppnp.2007.07.001](https://doi.org/10.1016/j.ppnp.2007.07.001)
- Boshkayev, K., Rueda, J. A., Ruffini, R., & Siutsou, I. 2013, *Astrophys. J.*, 762, 117, doi: [10.1088/0004-637X/762/2/117](https://doi.org/10.1088/0004-637X/762/2/117)
- Buonanno, A., Iyer, B., Ochsner, E., Pan, Y., & Sathyaprakash, B. S. 2009, *Phys. Rev. D*, 80, 084043, doi: [10.1103/PhysRevD.80.084043](https://doi.org/10.1103/PhysRevD.80.084043)
- Cutler, C., et al. 1993, *Phys. Rev. Lett.*, 70, 2984, doi: [10.1103/PhysRevLett.70.2984](https://doi.org/10.1103/PhysRevLett.70.2984)
- Damour, T., Iyer, B. R., & Sathyaprakash, B. S. 2001, *Phys. Rev. D*, 63, 044023, doi: [10.1103/PhysRevD.63.044023](https://doi.org/10.1103/PhysRevD.63.044023)
- Duguet, T., Bender, M., Ebran, J. P., Lesinski, T., & Somà, V. 2015, *Eur. Phys. J. A*, 51, 162, doi: [10.1140/epja/i2015-15162-4](https://doi.org/10.1140/epja/i2015-15162-4)
- Feynman, R. P., Metropolis, N., & Teller, E. 1949, *Phys. Rev.*, 75, 1561, doi: [10.1103/PhysRev.75.1561](https://doi.org/10.1103/PhysRev.75.1561)
- Flanagan, E. E., & Hinderer, T. 2008, *Phys. Rev. D*, 77, 021502, doi: [10.1103/PhysRevD.77.021502](https://doi.org/10.1103/PhysRevD.77.021502)
- Fortune, H. T. 2016, *Phys. Rev. C*, 94, 064307, doi: [10.1103/PhysRevC.94.064307](https://doi.org/10.1103/PhysRevC.94.064307)
- Fryer, C. L., Benz, W., Herant, M., & Colgate, S. A. 1999, *Astrophys. J.*, 516, 892, doi: [10.1086/307119](https://doi.org/10.1086/307119)
- Gasser, J., Sainio, M. E., & Svarc, A. 1988, *Nucl. Phys. B*, 307, 779, doi: [10.1016/0550-3213\(88\)90108-3](https://doi.org/10.1016/0550-3213(88)90108-3)
- Gibney, E. 2024, *Nature*, 625, 604, doi: <https://doi.org/10.1038/d41586-024-00254-x>
- Gong, Y., Luo, J., & Wang, B. 2021, *Nature Astron.*, 5, 881, doi: [10.1038/s41550-021-01480-3](https://doi.org/10.1038/s41550-021-01480-3)
- Guo, L.-J., Xiong, J.-Y., Ma, Y., & Ma, Y.-L. 2024, *Astrophys. J.*, 965, 47, doi: [10.3847/1538-4357/ad2e8d](https://doi.org/10.3847/1538-4357/ad2e8d)
- Harada, M., & Yamawaki, K. 2003, *Phys. Rept.*, 381, 1, doi: [10.1016/S0370-1573\(03\)00139-X](https://doi.org/10.1016/S0370-1573(03)00139-X)

- Hergert, H., Bogner, S. K., Morris, T. D., Schwenk, A., & Tsukiyama, K. 2016, *Phys. Rept.*, 621, 165, doi: [10.1016/j.physrep.2015.12.007](https://doi.org/10.1016/j.physrep.2015.12.007)
- Horowitz, C. J., Perez-Garcia, M. A., Berry, D. K., & Piekarewicz, J. 2005, *Phys. Rev. C*, 72, 035801, doi: [10.1103/PhysRevC.72.035801](https://doi.org/10.1103/PhysRevC.72.035801)
- Hu, W.-R., & Wu, Y.-L. 2017, *Natl. Sci. Rev.*, 4, 685, doi: [10.1093/nsr/nwx116](https://doi.org/10.1093/nsr/nwx116)
- Husa, S., Khan, S., Hannam, M., et al. 2016, *Phys. Rev. D*, 93, 044006, doi: [10.1103/PhysRevD.93.044006](https://doi.org/10.1103/PhysRevD.93.044006)
- Isoyama, S., Sturani, R., & Nakano, H. 2020, doi: [10.1007/978-981-15-4702-7\\_31-1](https://doi.org/10.1007/978-981-15-4702-7_31-1)
- Jenkins, E. E., & Manohar, A. V. 1991, *Phys. Lett. B*, 255, 558, doi: [10.1016/0370-2693\(91\)90266-S](https://doi.org/10.1016/0370-2693(91)90266-S)
- Jose, J., & Hernanz, M. 1998, *Astrophys. J.*, 494, 680, doi: [10.1086/305244](https://doi.org/10.1086/305244)
- Kashiyama, K., Ioka, K., & Mészáros, P. 2013, *Astrophys. J. Lett.*, 776, L39, doi: [10.1088/2041-8205/776/2/L39](https://doi.org/10.1088/2041-8205/776/2/L39)
- Katz, B., & Dong, S. 2012. <https://arxiv.org/abs/1211.4584>
- Kawaguchi, K., Kiuchi, K., Kyutoku, K., et al. 2018, *Phys. Rev. D*, 97, 044044, doi: [10.1103/PhysRevD.97.044044](https://doi.org/10.1103/PhysRevD.97.044044)
- Korol, V., et al. 2020, *Astron. Astrophys.*, 638, A153, doi: [10.1051/0004-6361/202037764](https://doi.org/10.1051/0004-6361/202037764)
- Lesinski, T., Bennaceur, K., Duguet, T., & Meyer, J. 2006, *Phys. Rev. C*, 74, 044315, doi: [10.1103/PhysRevC.74.044315](https://doi.org/10.1103/PhysRevC.74.044315)
- Li, Y.-L., Ma, Y.-L., & Rho, M. 2017, *Phys. Rev. D*, 95, 114011, doi: [10.1103/PhysRevD.95.114011](https://doi.org/10.1103/PhysRevD.95.114011)
- Luo, J., et al. 2016, *Class. Quant. Grav.*, 33, 035010, doi: [10.1088/0264-9381/33/3/035010](https://doi.org/10.1088/0264-9381/33/3/035010)
- Luo, Z., Guo, Z., Jin, G., Wu, Y., & Hu, W. 2020, *Results in Physics*, 16, 102918, doi: <https://doi.org/10.1016/j.rinp.2019.102918>
- Luo, Z., Wang, Y., Wu, Y., Hu, W., & Jin, G. 2021, *PTEP*, 2021, 05A108, doi: [10.1093/ptep/ptaa083](https://doi.org/10.1093/ptep/ptaa083)
- Ma, Y., & Ma, Y.-L. 2024, *Phys. Rev. D*, 109, 074022, doi: [10.1103/PhysRevD.109.074022](https://doi.org/10.1103/PhysRevD.109.074022)
- Ma, Y.-L., & Rho, M. 2017, *Sci. China Phys. Mech. Astron.*, 60, 032001, doi: [10.1007/s11433-016-0497-2](https://doi.org/10.1007/s11433-016-0497-2)
- McNeill, L. O., Mardling, R. A., & Müller, B. 2020, *Mon. Not. Roy. Astron. Soc.*, 491, 3000, doi: [10.1093/mnras/stz3215](https://doi.org/10.1093/mnras/stz3215)
- Moore, C. J., Cole, R. H., & Berry, C. P. L. 2015, *Class. Quant. Grav.*, 32, 015014, doi: [10.1088/0264-9381/32/1/015014](https://doi.org/10.1088/0264-9381/32/1/015014)
- National Nuclear Data Center. 2024, NuDat database, <https://www.nndc.bnl.gov/nudat/>
- Niemeyer, J. C., & Woosley, S. E. 1997, *Astrophys. J.*, 475, 740, doi: [10.1086/303544](https://doi.org/10.1086/303544)
- Oppenheimer, J. R., & Volkoff, G. M. 1939, *Phys. Rev.*, 55, 374, doi: [10.1103/PhysRev.55.374](https://doi.org/10.1103/PhysRev.55.374)
- Pössel, M. 2010, *Einstein Online*, 4, 1003
- Rosswog, S., Kasen, D., Guillochon, J., & Ramirez-Ruiz, E. 2009, *Astrophys. J. Lett.*, 705, L128, doi: [10.1088/0004-637X/705/2/L128](https://doi.org/10.1088/0004-637X/705/2/L128)
- Rotondo, M., Rueda, J. A., Ruffini, R., & Xue, S.-S. 2011a, *Phys. Rev. D*, 84, 084007, doi: [10.1103/PhysRevD.84.084007](https://doi.org/10.1103/PhysRevD.84.084007)
- Rotondo, M., Rueda, J. A., Ruffini, R., & Xue, S. S. 2011b, *Phys. Rev. C*, 83, 045805, doi: [10.1103/PhysRevC.83.045805](https://doi.org/10.1103/PhysRevC.83.045805)
- Ruiter, A. J., Belczynski, K., Benacquista, M., Larson, S. L., & Williams, G. 2010, *Astrophys. J.*, 717, 1006, doi: [10.1088/0004-637X/717/2/1006](https://doi.org/10.1088/0004-637X/717/2/1006)
- Salpeter, E. E. 1961, *Astrophys. J.*, 134, 669, doi: [10.1086/147194](https://doi.org/10.1086/147194)
- Saumon, D., Blouin, S., & Tremblay, P.-E. 2022, *Phys. Rept.*, 988, 1, doi: [10.1016/j.physrep.2022.09.001](https://doi.org/10.1016/j.physrep.2022.09.001)
- Scherer, S. 2010, *Prog. Part. Nucl. Phys.*, 64, 1, doi: [10.1016/j.ppnp.2009.08.002](https://doi.org/10.1016/j.ppnp.2009.08.002)
- Serot, B. D., & Walecka, J. D. 1986, *Adv. Nucl. Phys.*, 16, 1 —. 1997, *Int. J. Mod. Phys. E*, 6, 515, doi: [10.1142/S0218301397000299](https://doi.org/10.1142/S0218301397000299)
- Shen, H., Toki, H., Oyamatsu, K., & Sumiyoshi, K. 1998, *Nucl. Phys. A*, 637, 435, doi: [10.1016/S0375-9474\(98\)00236-X](https://doi.org/10.1016/S0375-9474(98)00236-X)
- Stoitsov, M., Kortelainen, M., Bogner, S. K., et al. 2010, *Phys. Rev. C*, 82, 054307, doi: [10.1103/PhysRevC.82.054307](https://doi.org/10.1103/PhysRevC.82.054307)
- Sugahara, Y., & Toki, H. 1994, *Nucl. Phys. A*, 579, 557, doi: [10.1016/0375-9474\(94\)90923-7](https://doi.org/10.1016/0375-9474(94)90923-7)
- Tamanini, N., & Danielski, C. 2019, *Nature Astron.*, 3, 858, doi: [10.1038/s41550-019-0807-y](https://doi.org/10.1038/s41550-019-0807-y)
- Tolman, R. C. 1939, *Phys. Rev.*, 55, 364, doi: [10.1103/PhysRev.55.364](https://doi.org/10.1103/PhysRev.55.364)
- Toonen, S., Nelemans, G., & Portegies Zwart, S. 2012, *Astron. Astrophys.*, 546, A70, doi: [10.1051/0004-6361/201218966](https://doi.org/10.1051/0004-6361/201218966)
- Tremblay, P.-E., Gentile-Fusillo, N., Raddi, R., et al. 2016, *Monthly Notices of the Royal Astronomical Society*, stw2854
- Walecka, J. D. 1974, *Annals Phys.*, 83, 491, doi: [10.1016/0003-4916\(74\)90208-5](https://doi.org/10.1016/0003-4916(74)90208-5)
- Watanabe, G., Iida, K., & Sato, K. 2000, *Nucl. Phys. A*, 676, 455, doi: [10.1016/S0375-9474\(00\)00197-4](https://doi.org/10.1016/S0375-9474(00)00197-4)
- Weinberg, S. 1979, *Physica A*, 96, 327, doi: [10.1016/0378-4371\(79\)90223-1](https://doi.org/10.1016/0378-4371(79)90223-1)
- . 1990, *Phys. Lett. B*, 251, 288, doi: [10.1016/0370-2693\(90\)90938-3](https://doi.org/10.1016/0370-2693(90)90938-3)

Wolz, A., Yagi, K., Anderson, N., & Taylor, A. J. 2020,  
Mon. Not. Roy. Astron. Soc., 500, L52,  
doi: [10.1093/mnrasl/slaa183](https://doi.org/10.1093/mnrasl/slaa183)

Xia, C.-J., Maruyama, T., Li, A., et al. 2022, Commun.  
Theor. Phys., 74, 095303, doi: [10.1088/1572-9494/ac71fd](https://doi.org/10.1088/1572-9494/ac71fd)

You, H.-S., Sun, H., Li, H.-B., Xia, C.-J., & Xu, R.-X. 2024.  
<https://arxiv.org/abs/2406.00613>

Yu, S., & Jeffery, C. S. 2010, Astron. Astrophys., 521, A85,  
doi: [10.1051/0004-6361/201014827](https://doi.org/10.1051/0004-6361/201014827)

Zuo, Z. W., Pei, J. C., Xiong, X. Y., & Zhu, Y. 2018, Chin.  
Phys. C, 42, 064106, doi: [10.1088/1674-1137/42/6/064106](https://doi.org/10.1088/1674-1137/42/6/064106)